ACE2 is required for daughter cell-specific G_1 delay in *Saccharomyces cerevisiae*

Tracy L. Laabs*†, David D. Markwardt*†, Matthew G. Slattery*, Laura L. Newcomb‡, David J. Stillman§, and Warren Heideman*‡¶

*School of Pharmacy and ‡Department of Biomolecular Chemistry, University of Wisconsin, Madison, WI 53705; and §Department of Pathology, University of Utah, Salt Lake City, UT 84112

Communicated by Henry R. Bourne, University of California, San Francisco, CA, June 26, 2003 (received for review September 27, 2002)

Saccharomyces cerevisiae **cells reproduce by budding to yield a mother cell and a smaller daughter cell. Although both mother and daughter begin G_1 simultaneously, the mother cell progresses through G_1 more rapidly. Daughter cell G_1 delay has long been thought to be due to a requirement for attaining a certain critical cell size before passing the commitment point in the cell cycle known as START. We present an alternative model in which the daughter cell-specific Ace2 transcription factor delays G_1 in daughter cells. Deletion of *ACE2* produces daughter cells that proceed through G_1 at the same rate as mother cells, whereas a mutant Ace2 protein that is not restricted to daughter cells delays G_1 equally in both mothers and daughters. The differential in G_1 length between mothers and daughters requires the Cln3 G_1 cyclin, and *CLN3*-GFP reporter expression is reduced in daughters in an *ACE2*-dependent manner. Specific daughter delay elements in the *CLN3* promoter are required for normal daughter G_1 delay, and these elements bind to an unidentified 127-kDa protein. This DNA-binding activity is enhanced by deletion of *ACE2*. These results support a model in which daughter cell G_1 delay is determined not by cell size but by an intrinsic property of the daughter cell generated by asymmetric cell division.**

In the budding yeast *Saccharomyces cerevisiae*, mother and daughter cells spend different lengths of time in G_1 before entering S phase. The larger mother cell progresses through G_1 relatively quickly, whereas the smaller daughter cell is delayed in G_1.

The Cln3 G_1 cyclin promotes progression through G_1 (1, 2). Multiple signal transduction pathways that regulate the rate of G_1 progression converge to regulate Cln3 transcription, translation, stability, and activity. Mating pheromone and osmotic shock arrest cells in G_1 in part by decreasing the activity of the Cln3/Cdc28 kinase complex (3–5). A leaky scanning mechanism involving a short upstream ORF (6) makes Cln3 translation extremely sensitive to the rate of protein synthesis: a 50% decrease in protein synthesis produces a 10-fold fall in Cln3 protein levels (7). This mechanism probably accounts for regulation of Cln3 translation by the Tor and protein kinase A pathways (7, 8). Nitrogen starvation also down-regulates Cln3 translation and stability (9). *CLN3* transcription is maintained throughout the cell cycle but displays some cell cycle periodicity that depends on early cell cycle boxes (ECB) sites upstream of the *CLN3* promoter (10, 11). Glucose media induce *CLN3* transcription and promote rapid G_1 progression (12). Glucose induction of *CLN3* requires glycolysis but not cell cycle progression and is not affected by mutations in the well characterized glucose repression or induction pathways (13, 14). Azf1, a glucose-activated transcription factor, binds to repeated elements in the *CLN3* promoter (15, 16). Thus, *CLN3* is an integrator for signals that regulate the rate of G_1 progression in *S. cerevisiae*.

The classical explanation for daughter cell G_1 delay is the critical size model, in which daughter cells remain in G_1 until they reach a cell size that triggers entry into S phase (17). In this model, the essential difference between mother and daughter is cell size. Shortly after this model was proposed, Wheals' group (18–20) published a set of studies indicating that the critical size model does not adequately explain yeast cell cycle control. Perhaps their most striking finding was a size-independent component of daughter cell G_1 delay (18, 19). This size-independent G_1 delay in daughters indicates that at least part of the daughter cell G_1 delay is an intrinsic property of the daughter cell.

More recent work has established several mechanisms that produce differential gene expression between mother and daughter cells. The *HO* gene is expressed exclusively in mother cells (21). *ASH1* mRNA is transported into the growing bud and accumulates only in daughter cells, where the Ash1 protein functions to block *HO* expression (22–24). In addition to Ash1, the Ace2 transcription factor accumulates exclusively in daughter cells (25, 26), and Ace2 target genes are expressed only in daughters (25). These results, demonstrating a daughter-specific pattern of gene expression, provide a conceptual framework to explain the intrinsic G_1 delay in daughter cells.

We present work based on the hypothesis that daughter cell G_1 delay depends on the specific localization of Ace2 to the daughter cell. In this model, daughter cell G_1 delay would be determined not by cell size but by the asymmetric distribution of Ace2 between mother and daughter cells. We report that Ace2 delays G_1 in daughter cells. Deletion of *ACE2* produces daughter cells that proceed through G_1 at the same rate as mother cells. In addition, an *ACE2* (G128E) mutation that allows Ace2 to function in both mothers and daughters prolongs G_1 in mothers, so that mother/daughter pairs proceed through G_1 at the same rate. Ace2 acts as a negative regulator of *CLN3* expression in daughter cells through an indirect mechanism.

Methods

Yeast Strains and Growth Conditions. Yeast were grown in YEPD media (1% yeast extract/2% peptone/2% glucose) and SD media (0.67% yeast nitrogen base/2% glucose) with auxotrophic supplements. Strains are listed in Table 2, which is published as supporting information on the PNAS web site, www.pnas.org.

Mutation of the *CLN3* daughter delay elements (DDEs) is described in *Supporting Text*, which is published as supporting information on the PNAS web site. The altered DDE sequences are as follows: DDE1-TTCCAGTCTATC; DDE2-TCCGCATTTCTC; DDE3-TCGCCAATATCT; DDE4-AAGTCTCCCTCT. The mutations were confirmed by sequencing.

Plasmids. Plasmids expressing *CLN3* from its own promoter were, or were derived from, pKL001 and pKL034 (27), which express *CLN3* from the −930/0 fragment of the *CLN3* promoter. Plasmids p414ADH, p424ADH, and p414TEF (28) were used to

Abbreviation: DDE, daughter delay element.

†T.L.L. and D.D.M. contributed equally to this work.

¶To whom correspondence should be addressed at: School of Pharmacy, University of Wisconsin, 777 Highland Avenue, Madison, WI 53705. E-mail: wheidema@facstaff.wisc.edu.

express *CLN3* from the *ADH1* and *TEF1* promoters and were gifts from M. Funk (Institute of Molecular Biology and Tumour Research, Philipps-Universität Marburg, Marburg, Gemany). Plasmid construction is described in *Supporting Text*.

Time-Lapse Microscopy and Cell Size Determination. Strains were collected in log phase, transferred to SD-agarose slabs with coverslips, and grown at 30°C for observation at 10-min intervals. After formation of daughter cells, the next budding event was scored for a mother/daughter pair as simultaneous if both cells showed the first sign of bud emergence at the same time point. Mother budding first was scored if a bud was identified forming on the mother cell with no observable bud on the daughter cell. Daughter budding first was scored if a bud was observed forming on a daughter cell with no identifiable bud on the mother cell. Micrographs were measured by using NIH IMAGE Ver. 1.62 to determine cell volume at bud emergence by using the formula: volume = $(\pi/6)ab^2$, where a is the major axis length, and b is the length of the minor axis (18). For both determinations, at least six sets of samples with $n = 20–30$ cells each were scored for each strain. Population cell size distributions were measured with a Coulter Counter Model Z2 (Beckman Coulter) by using a 70-μm aperture calibrated with 3-μm latex beads.

GFP. GFP fluorescence was measured by microscopy by using a Zeiss Axioplan 2 microscope with a ×100 oil immersion objective, equipped with a Hamamatsu ORCA-ER (Hamamatsu Photonics, Hamamatsu City, Japan) cooled charge-coupled device camera and recorded as TIFF files. NIH IMAGE Ver. 1.62 was used to integrate fluorescence intensity in mother/daughter pairs after subtracting the background signal measured in the adjacent area. For fluorescence, 300-msec exposures were used. Background fluorescence in control cells without GFP plasmid was undetectable at this exposure. The ratio of fluorescence in the mother over that in the daughter was calculated for each pair and averaged. Values are the averages from eight groups of eight pairs in each group. Separation of mother and daughter cells was determined by observation with differential interface contrast microscopy optics by using the methods described by Lord and Wheals (18). Pairs were chosen in which clear septation was visible; in addition, many of the pairs contained at least one budded cell, clearly indicative of completed mother/daughter separation.

RNA Preparation and Northern Blotting. Total yeast RNA was isolated and separated by formaldehyde gel electrophoresis, blotted, and probed as described (7).

Gel-Shift Assays. Gel shifts were performed as described (16). The probe was a double-stranded synthetic oligonucleotide (5′-GGA TTT AAC GTA TCC ATT GCA TTT CCT CAT TCG GTT TAA CTC CTC T-3′).

Southwestern Blots. The protocol described by Parviz *et al.* (15) was used for Southwestern blot preparation and probing with the fragment described above for the gel-shift experiments. Blots and gels were exposed by using a Molecular Dynamics PhosphorImager.

Results

If daughter cell G_1 length is determined by daughter-specific components rather than by daughter cell size, then blocking the molecular processes that specify differences between mothers and daughters should produce mother/daughter pairs with equivalent G_1 lengths. We used time-lapse experiments to determine whether mutations in *ACE2* cause simultaneous mother/daughter budding. In these experiments, we followed the formation of mother/daughter pairs and the subsequent

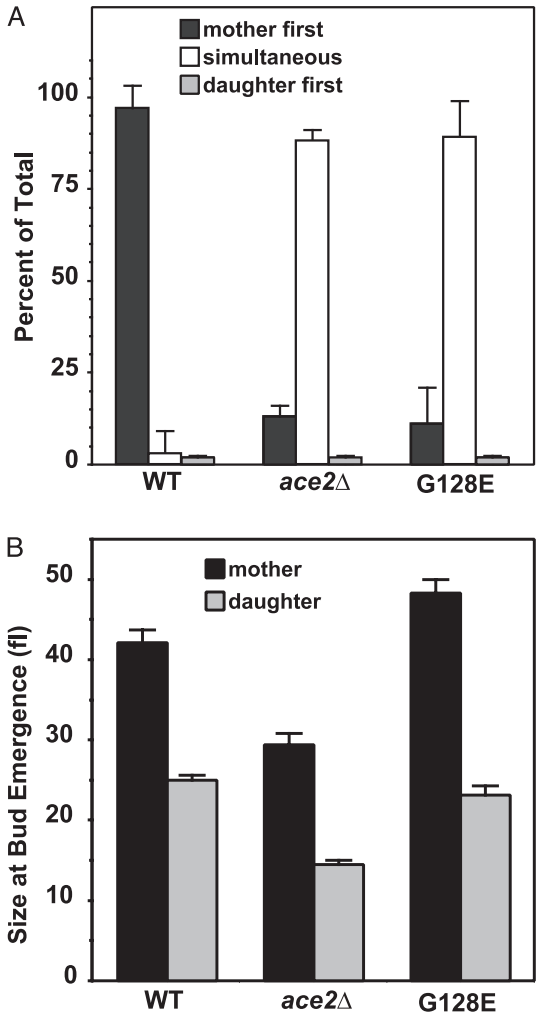

Fig. 1. *ACE2* and daughter cell G_1 delay. (*A*) Time-lapse experiments. Wild-type (BY4741), *ace2*Δ (4088), and *ace2*Δ::ACE2G128E (TTL53) cells were grown as described in *Methods*. Formation of mother/daughter pairs was followed by using a ×40 objective, and pairs were scored as budding simultaneously if buds appeared on both mother and daughter in a pair that had been unbudded at the previous time point. (*B*) Images of newly budded cells were measured for long and short axis lengths by using NIH IMAGE Ver. 1.62, and cell volumes were calculated as described in *Methods*. Error bars indicate SEM.

emergence of new buds as mother and daughter completed the next G_1 phase. For wild-type strains, the mother cell budded ahead of the daughter cell in >95% of the pairs examined (Fig. 1*A*). In contrast, we found that *ace2*Δ mothers and daughters budded simultaneously in ≈90% of the pairs examined, showing that the difference in G_1 length between mothers and daughters depends on *ACE2*.

Our experiments suggest that *ace2*Δ daughters have lost G_1 delay and proceed through G_1 like mother cells. We measured cell size at bud emergence as a measure of relative G_1 length (Fig. 1*B*). As expected, *ace2*Δ daughter cells bud at a smaller size than wild-type daughters, indicative of a shortened G_1. Because *ace2*Δ mother cells start out smaller than normal at the first bud emergence, they might be expected to remain smaller than their wild-type counterpart at subsequent rounds of bud formation. Consistent with this idea, deletion of *ACE2* also decreased the average size of mother cells at bud emergence.

The converse situation, in which mother cells behave like daughters, is found in cells carrying a dominant *ACE2* (G128E) mutation (25, 29), encoding an Ace2 protein not restricted to

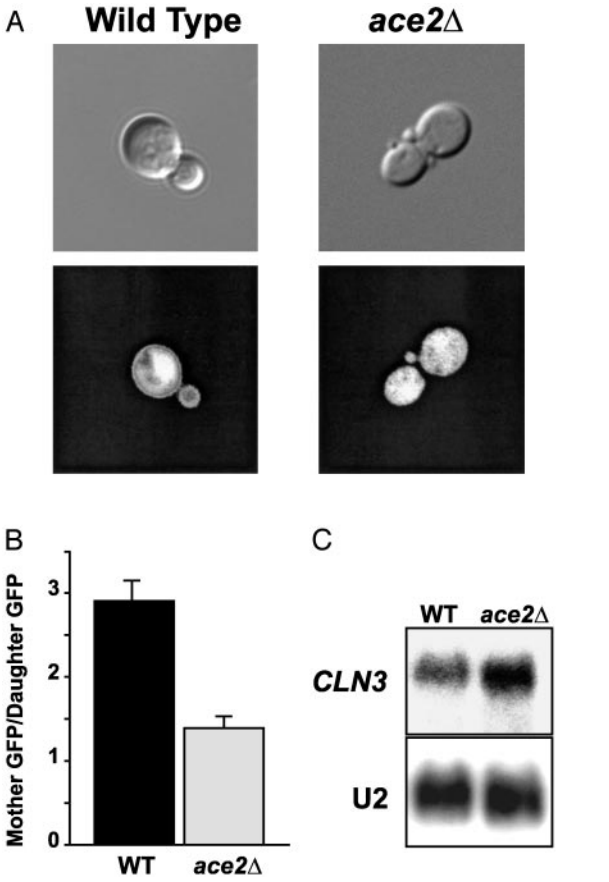

Fig. 2. *ACE2* and *CLN3* expression in daughter cells. (*A*) Wild-type and *ace2*Δ cells were transformed with the P_{CLN3}-GFP reporter and examined in log phase growth by using a ×100 objective with differential interference contrast microscopy (*Upper*) and fluorescence (*Lower*). (*B*) NIH IMAGE Ver. 1.62 was used to measure fluorescence in TIFF files generated from mother/daughter pairs, as described in *Methods*, to yield a ratio of fluorescence in mothers over that in daughters. Average values from eight groups of eight pairs each are presented for each strain. Error bars indicate standard error of the mean. (*C*) Wild-type and *ace2*Δ cells were grown in YEPD media to a density of 1 OD_{660}, and samples were collected for RNA preparation and Northern blotting with a *CLN3* probe. U2 RNA was probed as a loading and transfer control.

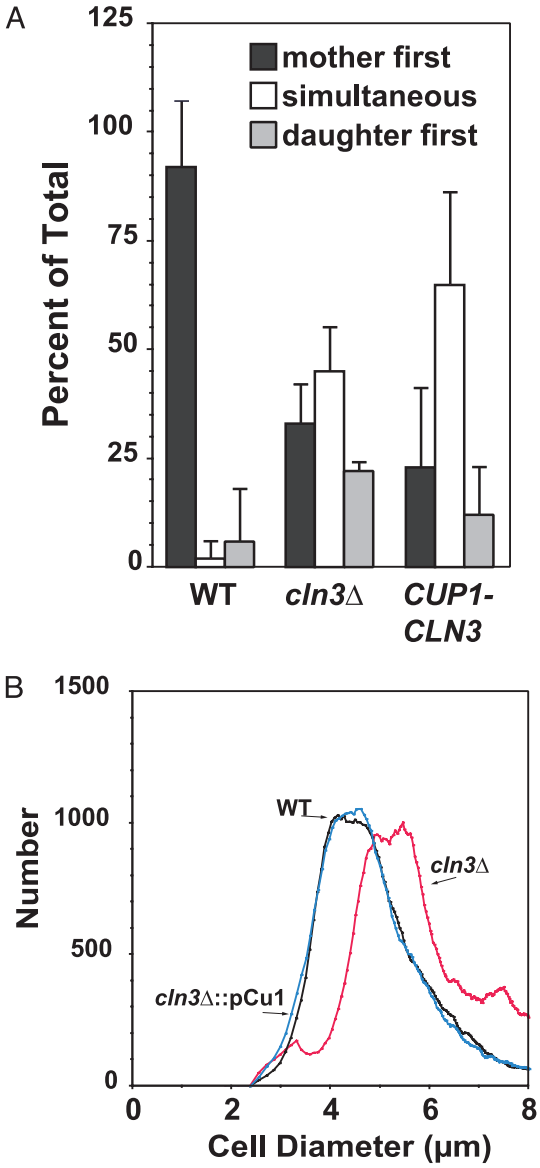

Fig. 3. *CLN3* regulation is necessary for daughter G_1 delay. (*A*) Wild-type (DS10), *cln3*Δ (DM15), and *cln3*Δ::P_{CUP1}-*CLN3* (DM16) cells were grown on SD agar slabs for time-lapse scoring as described in Fig. 1. (*B*) The strains were grown to a density of 0.5 OD_{660} and collected at log phase for size measurements with a Coulter Counter Channelizer (Beckman Coulter) calibrated with 3-μm latex beads. WT, black trace; *cln3*Δ, red trace; *cln3*Δ::pCu1, blue trace.

daughters (25, 29). In our model, Ace2 function in both mother and daughter cells should cause both mothers and daughters to be delayed in G_1 equally. As predicted, the *ACE2* (G128E) mutation also produces simultaneous budding in mother/daughter pairs (Fig. 1*A*).

The presence of Ace2 protein in *ACE2* (G128E) mother cells should prolong G_1 in mothers to match daughter G_1 length. As expected, we found that the *ACE2* (G128E) mutation increased the cell size at bud emergence for mother cells, indicating a prolonged G_1. Because Ace2 is normally present in daughters, we expected no effect of the ACE2 (G128E) mutation on daughter cell G_1 length. Daughter cell size at bud emergence remained unchanged in the *ACE2* (G128E) mutants (Fig. 1*B*).

Ace2 and *CLN3*. Because *CLN3* promotes passage through G_1, a possible model is that Ace2 decreases expression of *CLN3* in daughters, thereby delaying progress through G_1. As a test, we constructed a GFP reporter driven by a *CLN3* promoter fragment (from −751 to + 1). In wild-type cells, this reporter displayed a modest but consistent decrease in expression in daughter cells compared with mothers (Fig. 2*A*). This difference in *CLN3* expression may be sufficient to explain the difference in G_1 length between mothers and daughters. We found that the difference in *CLN3*-GFP fluorescence between mothers and daughters was abolished in an *ace2*Δ strain, indicating that Ace2 is necessary for the decreased *CLN3*-GFP expression in daughters.

We used fluorescence microscopy and NIH IMAGE to quantitate the difference in GFP levels between mother and daughter cells in wild-type and *ace2* mutants. We chose this approach in place of flow cytometry because of the clumping phenotype of *ace2*Δ mutants. We observed a difference in overall GFP signal between mothers and daughters. This difference was largely abolished in the *ace2*Δ mutants (Fig. 2*B*).

A Northern blot shows that *CLN3* mRNA levels increase overall when *ACE2* is deleted (Fig. 2*C*). Taken together, these results indicate that the presence of Ace2 in daughter cells produces a decrease in *CLN3* expression.

Table 1. *CLN3* expression and cell size

Strain	Simultaneous budding	Cell size	Relative expression
Wild type (DS10)	−	42.5 ± 0.3	
*cln3*Δ (DM16)	+	57.6 ± 0.4	
CLN3-DDEΔ (TL70)	+	44.0 ± 2.9	
*cln3*Δ::CEN P_{CLN3}-*CLN3* (TL28)	−	50.1 ± 0.6	
*cln3*Δ::2μ P_{CLN3}-*CLN3* (TL30)	−	38.2 ± 1.0	
*cln3*Δ::2μ P_{ADH1}-*CLN3* (TL50)	+	37.6 ± 0.3	90
*cln3*Δ CEN P_{TEF1}-*CLN3* (TL32)	+	39.9 ± 0.6	50
*cln3*Δ::CEN P_{ADH1}-*CLN3* (TL49)	+	47.8 ± 0.7	3

Cells were grown in selective medium overnight and transferred to YEPD media for budding measurements and size measurements, as described in *Methods*. Relative expression levels of 2μ *ADH1*, CEN *TEF1*, and CEN *ADH1* are from Mumberg *et al.* (28).

If Ace2 down-regulates *CLN3* in daughters to cause a G_1 delay, then *CLN3* should be necessary for the normal difference in G_1 length between mothers and daughters. We found that *CLN3* deletion increased the fraction of mother/daughter pairs that budded simultaneously (Fig. 3*A*). This result indicates that *CLN3* plays a role in this process. The effect of *CLN3* deletion was not as dramatic as that seen with the *ace2*Δ strain, suggesting that *CLN3* does not completely account for daughter cell G_1 delay. Deletion of *BCK2*, a gene thought to play a parallel role to that of *CLN3* in G_1 regulation (30–32), had no effect on the budding pattern (not shown).

CLN3 Regulatory Sequences. Ace2 might regulate *CLN3* expression via 5′ elements upstream of the *CLN3* ORF. There are potential Ace2-binding sites in the *CLN3* promoter at positions −1185 and −1016. To test whether *ACE2* affects G_1 length via the *CLN3* promoter, we expressed *CLN3* from other promoters. *cln3*Δ cells carrying a plasmid in which *CLN3* is expressed from the *CUP1* promoter had a budding phenotype similar to that seen in *ACE2* mutants, in which mothers and daughters budded simultaneously (Fig. 3*A*). This result demonstrates that *CLN3* 5′ regulatory sequences are required to produce differential G_1 length between mothers and daughters.

Simultaneous mother/daughter budding was not simply the result of *CLN3* overexpression. Increased *CLN3* expression from a multicopy plasmid does not result in simultaneous mother/daughter budding, although it does shorten G_1 in both mother and daughter cells, producing a decrease in modal cell size (Table 1). In contrast, expression of *CLN3* from heterologous promoters invariably produced simultaneous budding, regard-

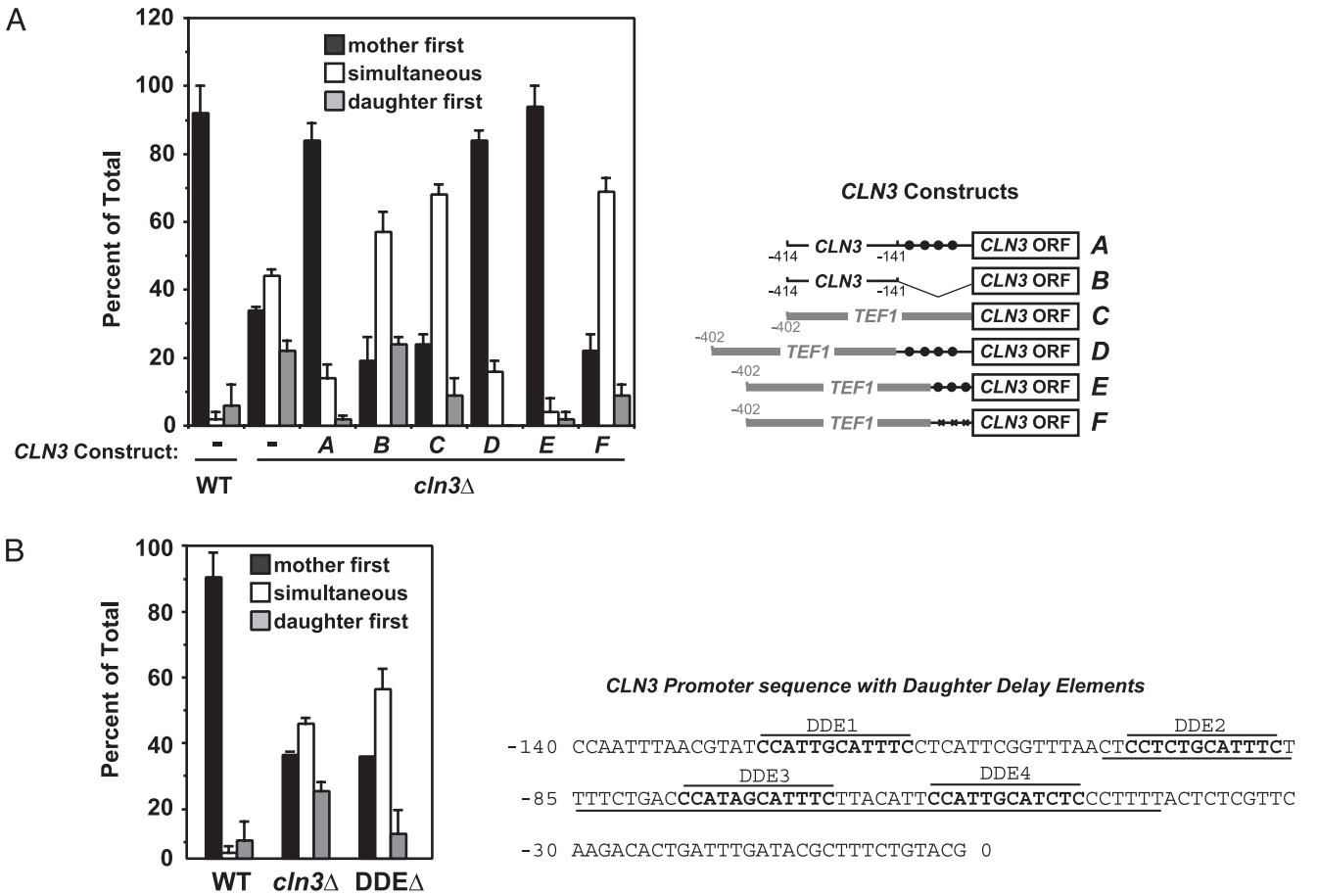

Fig. 4. Elements in the *CLN3* promoter mediate normal G_1 delay in daughter cells. (*A*) Wild-type (DS10), *cln3*Δ (DM15), and *cln3*Δ cells carrying various centromeric plasmids expressing *CLN3* from different test promoters were grown for time-lapse experiments as described for Fig. 1. Maps indicating the arrangement of the *CLN3* expression constructs are shown (*Right*), with *TEF1* sequence indicated by gray and DDEs indicated by filled circles. Promoter arrangements were: A, TL29, the −414/0 region of the *CLN3* promoter; B, TL55, the −414−141 region of the *CLN3* promoter; C, TL32, the −402/0 fragment from the *TEF1* promoter; D, TL60, the *TEF1* promoter with the −140/0 region of the *CLN3* promoter; E, TL61, the *TEF1* promoter with the −100/−41 region of the *CLN3* promoter; *F*, TL62, the *TEF1* promoter with the −100/−41 region of the *CLN3* promoter in which the DDEs had been scrambled (indicated by Xs). (*B*) Wild-type (DS10), *cln3*Δ (DM15), and a strain carrying mutated DDEs upstream of the *CLN3* ORF (TL70) were grown for time-lapse experiments as described. The −140/0 sequence from the *CLN3* promoter is shown (*Right*) with DDEs indicated.

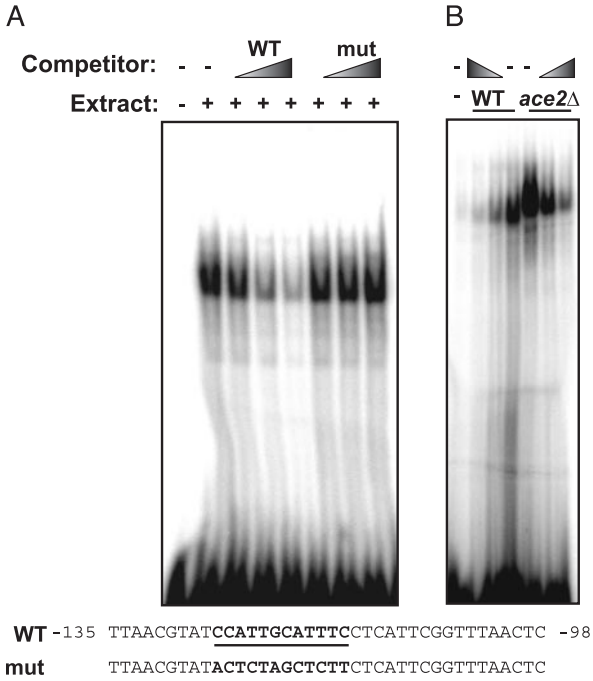

Fig. 5. DDEs in the *CLN3* promoter produce a specific gel-shift band. Gel-shift assays with 10-μg samples of yeast extract and the probe sequence indicated as wild type were performed as described in *Methods*. (*A*) Gel shift with wild-type extract and 10-, 25-, and 50-fold excess unlabeled wild-type (WT) or mutant (mut) competitor. (*B*) Gel shift with extracts from wild-type and *ace2*Δ cells.

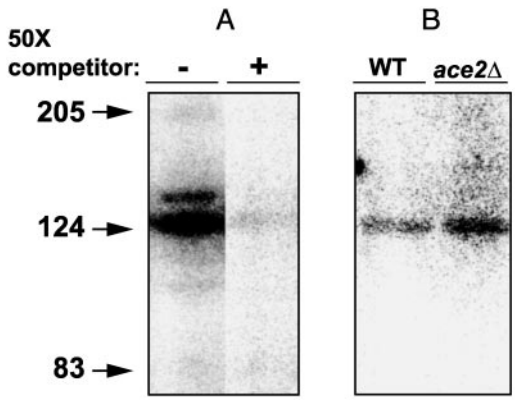

Fig. 6. A 126-kDA protein interacts with *CLN3* promoter elements. (*A*) Extracts from wild-type and *ace2*Δ cells were separated by SDS gel electrophoresis (50 μg per lane) and transferred to nitrocellulose as described in *Methods*. Radiolabeled wild-type oligo was used to probe the blot in the presence or absence of a 50-fold excess of unlabeled oligo. (*B*) Extracts from wild-type and *ace2*Δ cells were separated and probed as described for *A*. Prestained molecular weight standards were as follows: myosin, 206 kDa; β-galactosidase, 124 kDa; and BSA, 83 kDa.

less of effects on cell size (Table 1). Consistent with previous results (1, 2), we found that cell size was inversely proportional to the strength of the promoter driving *CLN3* expression. Interestingly, the cell size distribution of the *cln3*Δ cells expressing *CLN3* from the *CUP1* and *TEF1* promoter constructs was very close to that of wild type. These results indicate that a normal cell size distribution is possible in cultures where mothers and daughters bud simultaneously (Table 1 and Fig. 3*B*).

CLN3 promoter deletions were made to define regulatory regions required for G_1 delay in daughter cells. *CLN3* driven by a promoter fragment from −414 to 0 showed the normal mother-first budding pattern seen in wild-type cells, indicating that sequences within this region are sufficient to produce daughter cell G_1 delay (Fig. 4*A*). The −414/0 promoter construct does not contain the Ace2 consensus sites at positions −1185 and −1016. In contrast, the −414 to −141 *CLN3* promoter fragment did not produce normal budding, with mothers and daughters budding simultaneously, indicating that elements within the region from −140/0 are necessary for normal daughter G_1 delay.

As with all heterologous promoter constructs tested, expression of *CLN3* from the *TEF1* promoter produced simultaneous mother/daughter budding (Fig. 4). However, we found that insertion of the −140/0 *CLN3* promoter segment into the junction between the *TEF1* promoter and the *CLN3* ORF restored normal daughter cell G_1 delay. The −140/0 region contains four copies of a repeated element with a consensus sequence of CCATTGCATTTC. Inserting three of these repeated elements (the underlined sequence in Fig. 4) between the *TEF1* promoter and the *CLN3* ORF also produced normal daughter cell G_1 delay. In contrast, when we rearranged the bases within the repeated elements, the construct was no longer able to confer normal budding. We conclude that the repeated elements in the *CLN3* promoter play a role in daughter cell G_1 delay and refer to these sequences as daughter delay elements (DDEs).

Specific mutation of the *CLN3* DDEs in our wild-type strain produced a loss of daughter cell G_1 delay comparable to that seen with deletion of *CLN3* (Fig. 4*B*). However, in contrast to *CLN3* deletion, mutation of the DDEs affected only daughter G_1 delay and had little effect on the modal cell size of the population (Table 1). This result shows that the *CLN3* DDEs play an important role in daughter cell G_1 delay.

A gel shift using a probe containing the first of the DDEs produced a specific band that was more intense and retarded in mobility with *ace2*Δ mutant extract than with the wild-type extract (Fig. 5). This result indicates that the DDEs specifically interact with one or more proteins in yeast cell extracts, and that Ace2 alters the formation of the DDE–protein complex.

Southwestern blots demonstrated specific binding of labeled DDEs to a protein of ≈127 kDa (Fig. 6*A*). As with the gel-shift experiments, this band was more intense with extracts from an *ace2*Δ strain than with wild-type extracts (Fig. 6*B*).

Discussion

A Model for Daughter Cell G_1 Delay. Fig. 7 presents a model in which the exclusive presence of Ace2 in daughter cells inhibits *CLN3* expression, prolonging G_1 in daughters. Mothers and daughters

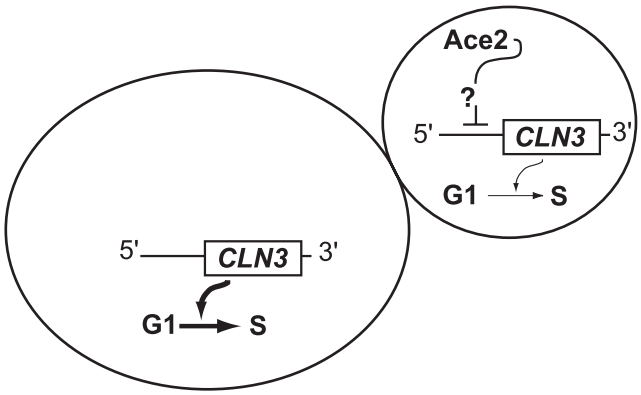

Fig. 7. Proposed model for daughter cell G_1 delay.

progress through G_1 simultaneously in the absence of Ace2 or when Ace2 is distributed to both mothers and daughters.

It is noteworthy that the model presented above contradicts the commonly held model in which daughter cells are delayed in G_1 until they reach the critical size for bud emergence. In the critical size model, the only distinction between mother and daughter is cell size. We propose that G_1 delay is not related to cell size but is specified by asymmetric distribution of regulatory components. Our model is supported by a set of experiments conducted by Wheals' group two decades ago. In examining populations of mother and daughter cells of equivalent size, Lord and Wheals (18, 19) reported that daughter cells have a substantially longer G_1 phase than mother cells, indicating that daughters have an intrinsic G_1 delay that is cell size independent. Our results provide a mechanism to explain the intrinsic delay.

We also sought evidence supporting the critical size model. Cells might sense size through the rate of protein synthesis (33), which is higher in larger than in smaller cells (34). Cln3 translation is especially sensitive to the rate of overall protein synthesis (6, 7), and decreased Cln3 translation in the daughter cells would prolong G_1. However, we found that deletion of the upstream ORF that links *CLN3* translation to the rate of protein synthesis failed to alter mother/daughter budding (not shown).

Two genome-wide screens for altered cell size in *S. cerevisiae* have recently been reported (35, 36). Although these mutants have been described as affecting the critical size for passing START, our results suggest that *S. cerevisiae* cells may not have a size checkpoint at all. Instead, we suggest that yeast cells maintain their size by coordinating the rate of cellular growth with the rate of progress through G_1. In this view, mutations that affect cell size have interrupted the balance between growth and progression through the cell cycle. Cln3/Cdc28 kinase activity is already known to be the target of a network of pathways that coordinate the rates of growth and G_1 progression, (3–7, 9, 13–16, 37, 38). The critical size model is undeniably elegant. However, evolutionary mechanisms may favor complexity over elegance.

CLN3 Regulation. Although we have shown that the *CLN3* DDEs are necessary and sufficient to produce daughter G_1 delay, the connection between Ace2 and *CLN3* is missing. Although many models are possible, perhaps the simplest one is that Ace2 inhibits an activator of *CLN3*. This latter model is attractive, because deletion of *ACE2* increases the formation of protein/DNA complexes in gel-shift and Southwestern assays.

Although our *CLN3*-GFP experiments indicate decreased reporter in daughters, these experiments pose difficulties in interpretation. Because mother cells had stronger signal intensity and a larger cross-sectional area than the daughters, the GFP signal represents both reporter concentration and quantity. It is not clear whether Cln3 concentration or amount is the most important factor in regulating G_1 length. In addition, plasmid distribution between mothers and daughters may be unequal. If so, the inequality depends largely on *ACE2*. We were unsuccessful with attempts to measure the signal from GFP integrated in place of the *CLN3* ORF.

G_1 Delay and Average Cell Size. Provided an appropriate level of *CLN3* expression exists, strains in which mothers and daughters bud simultaneously can have a normal average cell size. We found that replacing the *CLN3* 5′ regulatory sequences with heterologous promoters invariably produced simultaneous mother/daughter budding. However, G_1 length, and thus the average cell size of the population, depended on promoter strength, which is entirely consistent with a model in which Cln3 does not directly trigger START but instead governs G_1 progression as a rate.

We conclude that daughter G_1 delay is not required for a normal population cell size distribution. Instead, G_1 delay may function to allow daughter cells more time in which to expand their metabolic resources before turning to new cell production.

We thank Paul Ahlquist (University of Wisconsin, Madison, WI), Roger Brent (Molecular Sciences Institute, Berkeley, CA), Fred Cross (Rockefeller University, New York), Martin Funk (MediGene, Munich), and Emmett Schmidt (Massachusetts General Hospital, Boston) for providing yeast strains and plasmids; and Maureen Barr for useful discussions. We acknowledge the valuable assistance of M. Trudel, C. Carbonara, S. Guillen, A. Miller, D. Porcaro, E. Gizewski, N. Rosenberg, J. Renbourn, and P. Hish. This work was supported by National Science Foundation Grants 9982537 and 0235379 (to W.H.) and National Institutes of Health Grant GM48624 (to D.J.S.).

1. Cross, F. (1988) *Mol. Cell. Biol.* **8,** 4675–4684.
2. Nash, R., Tokiwa, G., Anand, S., Erickson, K. & Futcher, A. B. (1988) *EMBO J.* **7,** 4335–4346.
3. Jeoung, D.-I., Oehlen, L. J. W. M. & Cross, F. R. (1998) *Mol. Cell. Biol.* **18,** 433–441.
4. Tyers, M. & Futcher, B. (1993) *Mol. Cell. Biol.* **13,** 5659–5669.
5. Belli, G., Gari, E., Aldea, M. & Herrero, E. (2001) *Mol. Microbiol.* **39,** 1022–1035.
6. Polymenis, M. & Schmidt, E. V. (1997) *Genes Dev.* **11,** 2522–2531.
7. Hall, D. D., Markwardt, D. D., Parviz, F. & Heideman, W. (1998) *EMBO J.* **17,** 4370–4378.
8. Barbet, N. C., Schneider, U., Helliwell, S. B., Stansfield, I., Tuite, M. F. & Hall, M. N. (1996) *Mol. Biol. Cell* **7,** 25–42.
9. Gallego, C., Gari, E., Colomina, N., Herrero, E. & Aldea, M. (1997) *EMBO J.* **16,** 7196–7206.
10. Mai, B., Miles, S. & Breeden, L. L. (2002) *Mol. Cell. Biol.* **22,** 430–441.
11. McInerny, C. J., Partridge, J. F., Mikesell, G. E., Creemer, D. P. & Breeden, L. L. (1997) *Genes Dev.* **11,** 1277–1288.
12. Hubler, L., Bradshaw-Rouse, J. & Heideman, W. (1993) *Mol. Cell. Biol.* **13,** 6274–6282.
13. Parviz, F. & Heideman, W. (1998) *J. Bacteriol.* **180,** 225–230.
14. Newcomb, L. L., Diderich, J. A., Slattery, M. G. & Heideman, W. (2003) *Eukaryot. Cell* **2,** 143–149.
15. Parviz, F., Hall, D., Markwardt, D. & Heideman, W. (1998) *J. Bacteriol.* **180,** 4508–4515.
16. Newcomb, L. L., Hall, D. D. & Heideman, W. (2002) *Mol. Cell. Biol.* **22,** 1607–1614.
17. Johnston, G. C., Pringle, J. R. & Hartwell, L. H. (1977) *Exp. Cell Res.* **105,** 79–98.
18. Lord, P. & Wheals, A. (1981) *J. Cell Sci.* **50,** 361–376.
19. Lord, P. & Wheals, A. (1983) *J. Cell Sci.* **59,** 183–201.
20. Wheals, A. E. (1982) *Mol. Cell. Biol.* **2,** 361–368.
21. Sil, A. & Herskowitz, I. (1996) *Cell* **84,** 711–722.
22. Bertrand, E., Chartrand, P., Schaefer, M., Shenoy, S. M., Singer, R. H. & Long, R. M. (1998) *Mol. Cell* **2,** 437–445.
23. Bobola, N., Jansen, R. P., Shin, T. H. & Nasmyth, K. (1996) *Cell* **84,** 699–709.
24. Takizawa, P. A., Sil, A., Swedlow, J. R., Herskowitz, I. & Vale, R. D. (1997) *Nature* **389,** 90–93.
25. Colman-Lerner, A., Chin, T. E. & Brent, R. (2001) *Cell* **107,** 739–750.
26. Weiss, E. L., Kurischko, C., Zhang, C., Shokat, K., Drubin, D. G. & Luca, F. C. (2002) *J. Cell Biol.* **158,** 885–900.
27. Levine, K., Huang, K. & Cross, F. R. (1996) *Mol. Cell. Biol.* **16,** 6794–803.
28. Mumberg, D., Muller, R. & Funk, M. (1995) *Gene* **156,** 119–122.
29. Racki, W. J., Becam, A.-M., Nasr, F. & Herbert, C. J. (2000) *EMBO J.* **19,** 4524–4532.
30. Di Como, C. J., Chang, H. & Arndt, K. T. (1995) *Mol. Cell. Biol.* **15,** 1835–1846.
31. Epstein, C. B. & Cross, F. R. (1994) *Mol. Cell. Biol.* **14,** 2041–2047.
32. Wijnen, H. & Futcher, B. (1999) *Genetics* **153,** 1131–1143.
33. Moore, S. A. (1988) *J. Biol. Chem.* **263,** 9674–9681.
34. Woldringh, C. L., Huls, P. G. & Vischer, N. O. E. (1993) *J. Bacteriol.* **175,** 3174–3181.
35. Jorgensen, P., Nishikawa, J. L., Breitkreutz, B. J. & Tyers, M. (2002) *Science* **297,** 395–400.
36. Zhang, J., Schneider, C., Ottmers, L., Rodriguez, R., Day, A., Markwardt, J. & Schneider, B. L. (2002) *Curr. Biol.* **12,** 1992–2001.
37. Breeden, L. L. (2003) *Curr. Biol.* **13,** R31–R38.
38. Colomina, N., Gari, E., Gallego, C., Herrero, E. & Aldea, M. (1999) *EMBO J.* **18,** 320–329.